Multi-axial yield of aluminium alloy foams

V. S. Deshpande and N. A. Fleck
Engineering Department,University of Cambridge,
Trumpington Street, Cambridge CB2 1PZ, UK.

Abstract

A practical constitutive law is developed for multi-axial yielding of metallic foams. The constitutive law is motivated by triaxial experiments on Alporas and Duocel aluminium alloy foams, and has been implemented within the finite element code ABAQUS. We find that the yield surface is of quadratic shape in effective stress versus mean stress space, and that plastic flow is normal to the yield surface. The strain hardening behaviour is somewhat sensitive to the direction of stress path, with enhanced hardening observed under hydrostatic loading. The isotropic model presented here is adequate for loading paths which are not too far from proportional.

1 Introduction

The successful implementation of metallic foams requires the development of design methods based on engineering constitutive laws. A major aim of the current study is to provide a simple but reliable constitutive description of the yield behaviour of metallic foams.

Experimental data for the multi-axial yield of foamed metals are limited. The main contributions are those of Triantafillou et al. [1] and Gioux et al. [2]. Triantafillou et al. [1] conducted axisymmetric tests on an open-cell aluminium foam under combined axial tension and radial compression. Gioux et al. [2] reported yield data for closed and open cell aluminium foams under a variety of biaxial, shear and axisymmetric loadings. The presence of experimental scatter in these studies has made it difficult to establish the shape of the yield surfaces. Moreover, only the initial yield surface has been addressed. In many design situations, for example in energy absorbing devices, an understanding of the post-yield behaviour is essential.

Miller [3] proposed a continuum plasticity framework for metal foams. He modified the Drucker-Prager yield criterion and introduced three adjustable parameters to fit the yield surface to the then available experimental data viz. the uniaxial tensile and compressive yield points and lateral expansion rate or plastic Poisson's ratio of metal foams. He used the associated flow rule and a hardening law which scales with the uniaxial compressive behaviour of the foams to give a complete constitutive representation of the plastic behaviour.

In this paper the yield surfaces of an open cell and a closed cell aluminium foam are measured for axisymmetric compressive stress states. The evolution of the yield surfaces under uniaxial and hydrostatic compression is explored. A phenomenological isotropic constitutive model is then developed to model the observed behaviour.

J. Banhart, M.F. Ashby, N.A. Fleck: *Metal Foams and Porous Metal Structures.* © MIT Verlag (1999)

2 Experimental investigation

Two types of foams were investigated: Alporas and Duocel aluminium alloy foams. Alporas is a closed cell foam manufactured by the Shinko Wire Company, Amagasaki, Japan. The composition of the cell walls is Al-Ca 5-Ti 3 (wt %). Two relative densities, $\bar{\rho} = 8.4$ % and $\bar{\rho} = 16$ % were considered; for both densities the average cell size is approximately 4 mm. In the following we shall refer to the Alporas foam of density $\bar{\rho} = 8.4$ % as "low density Alporas foam" and the Alporas foam of density $\bar{\rho} = 16$ % as "high density Alporas foam". The open-cell Duocel foam manufactured by ERG, Oakland, CA, USA, is made from Al6101-T6 alloy. We tested a foam of relative density $\bar{\rho} = 7.0$ % and average cell size 2.5 mm. Further details on the structure, manufacturing processes and on the suppliers of these foams are given by Ashby et al. [4].

A brief description of the experiments conducted follows. A detailed description of the experimental apparatus and procedure is given in Deshpande and Fleck [5]. The initial yield surface was determined for the Alporas and Duocel foams by probing each specimen over a range of stress paths as sketched in Figure 1, using a triaxial cell. First, the specimen was pressurised until the offset axial plastic strain was 0.3 %. This pressure was taken as the yield strength under hydrostatic loading. The pressure was then decreased slightly and an axial displacement rate of 2×10^{-3} mm s^{-1} (strain rate of 4×10^{-5} s^{-1}) was applied until the offset axial strain had incremented by 0.3 %. The axial load was then removed and the pressure was decreased further, and the procedure was repeated. The procedure was continued until the uniaxial yield point was determined (ie. the stress state consisted of uniaxial stress with zero superimposed pressure). The yield points, defined at 0.3 % offset axial strain, were plotted in mean stress-effective stress space.

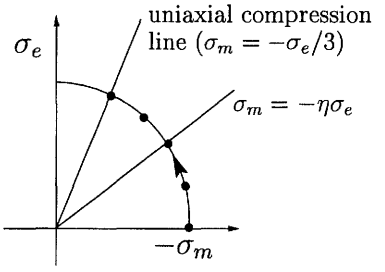

Figure 1: Probing of the yield surface.

In order to measure the evolution of the yield surface under uniaxial loading, the initial yield surface was probed as described above. The specimen was then compressed uniaxially to a desired level of axial strain and the axial load was removed; the yield surface was then re-probed. By repetition of this technique, the evolution of the yield surface under uniaxial loading was measured at a number of levels of axial strain from a single specimen. The evolution of the yield surface under hydrostatic loading was measured in a similar manner.

3 Experimental results

The uniaxial compressive responses of the Alporas and Duocel foams are shown in Figure 2, using the axes of axial Cauchy stress and true (logarithmic) axial strain. The Cauchy stress was calculated from the nominal uniaxial stress and the measured plastic Poisson's ratio values. Results from hydrostatic compression tests are included in Figure 2. In this case we take as axes the pressure and the true (logarithmic) volumetric strain. A comparison between the hydrostatic and uniaxial compression stress versus strain curves shows that the hardening rate under hydrostatic compression is much greater than the hardening rate under uniaxial compression for the high density Alporas foam ($\bar{\rho} = 16$ %). In contrast, the

hydrostatic and uniaxial hardening rates are comparable for the low density Alporas foam ($\bar{\rho} = 8.4$ %) and the Doucel foam ($\bar{\rho} = 7.0$ %).

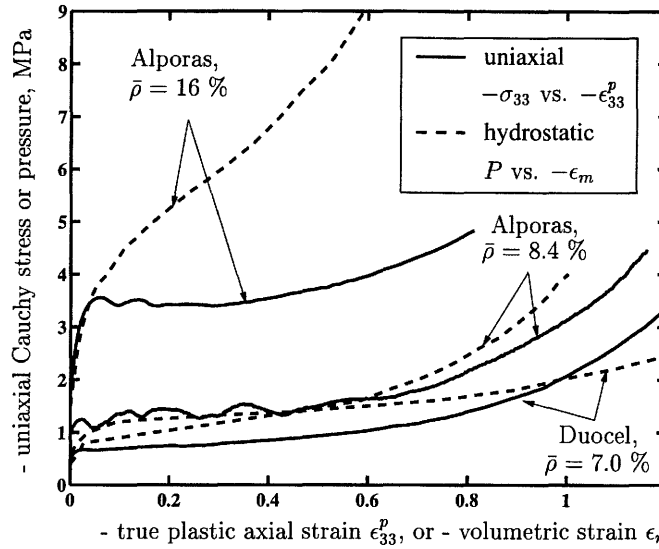

Figure 2: Uniaxial and hydrostatic compression stress-strain curves for the low and high density Alporas, and Duocel foams.

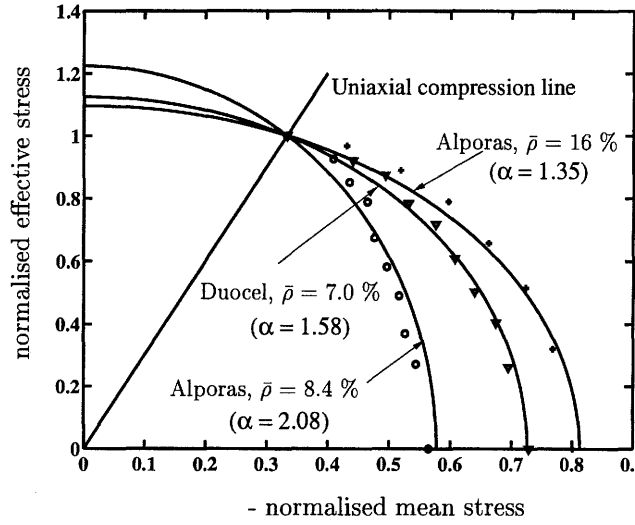

Figure 3: Initial yield surfaces of the low and high density Alporas, and Duocel foams. The stresses have been normalised by the uniaxial yield strength.

The initial yield surfaces for the three foams are plotted in Figure 3, using the axes of mean stress and effective stress. Both the mean stress and effective stress values have been normalised by the uniaxial yield strength of the respective specimen.

The evolution of the yield surface of the high density Alporas under uniaxial and hydrostatic compressive loading is shown in Figure 4. It is clear that the yield surfaces remain quadratic in shape and show no evidence of corner development at the loading point. Under uniaxial loading the yield surfaces evolve in approximately a geometrically self-similar manner (ie. their shapes do not change), while under hydrostatic loading the yield surfaces elongate along the hydrostatic axes. Yield surface evolution data for the low density Alporas and Duocel foams are given in Deshpande and Fleck [5].

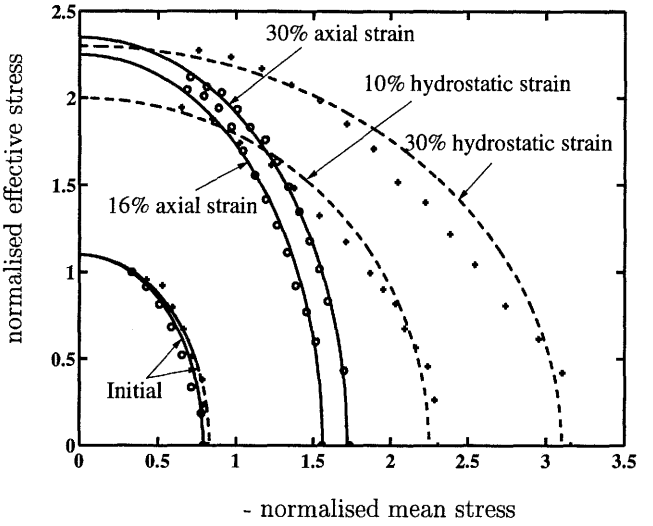

Figure 4: Evolution of the yield surface of the high density Alporas foam under uniaxial and hydrostatic loading. The stresses have been normalised by the initial uniaxial yield strength.

4 Constitutive modelling

In this section an isotropic constitutive model is developed for metallic foams, based on the experimental observations described above. It is assumed that the yield function Φ depends only on the first two stress invariants σ_m and σ_e and is independent of the third stress invariant $J_3 = (\sigma'_{ij}\sigma'_{jk}\sigma'_{ki})^{1/3}$; here the prime denotes the deviatoric part of the stress tensor. We shall also assume that the yield function is even in σ_m. This is supported by recent experimental studies as follows. Harte et al. [6] found that the uniaxial tensile yield strength is approximately equal to the uniaxial compressive yield strength for both Alporas and Duocel foams; Gioux et al. [2] measured the yield surface shapes of Alporas and Duocel foams and concluded that the asymmetry in shape with respect to mean stress is negligible.

We define a yield function Φ by

$$\Phi \equiv \hat{\sigma} - Y \leq 0, \tag{1}$$

where the equivalent stress $\hat{\sigma}$ is given by

$$\hat{\sigma}^2 = \frac{1}{\left[1+\left(\frac{\alpha}{3}\right)^2\right]}\left[\sigma_e^2 + \alpha^2\sigma_m^2\right]. \tag{2}$$

Here, $\sigma_e \equiv \sqrt{\frac{3}{2}\sigma'_{ij}\sigma'_{ij}}$ is the von Mises effective stress, $\sigma_m \equiv \sigma_{kk}/3$ is the mean stress, and the parameter α defines the shape of the yield surface. Again, a prime denotes the deviatoric quantity.

Equations (1) and (2) describe a yield surface of elliptical shape in (σ_m, σ_e) space, with a uniaxial yield strength (in tension and compression) of $\hat{\sigma}$, and a hydrostatic yield strength of $|\sigma_m| = \frac{\sqrt{1+(\alpha/3)^2}}{\alpha}\hat{\sigma}$. Thus, the parameter α defines the aspect ratio of the ellipse; in the limit $\alpha = 0$, $\hat{\sigma}$ reduces to σ_e and the von Mises yield criterion is recovered. Figure 3 shows that the yield surfaces defined by Equation 1 fit the experimental data for the three foams very well with appropriate choices for α.

The plastic strain rate $\dot{\epsilon}^p_{ij}$ is assumed to be normal to the yield surface (associated flow) and is given by

$$\dot{\epsilon}^p_{ij} = \frac{1}{H}\frac{\partial\Phi}{\partial\sigma_{ij}}\frac{\partial\Phi}{\partial\sigma_{kl}}\breve{\sigma}_{kl}, \tag{3}$$

where H is the hardening modulus and $\breve{\sigma}_{ij}$ is the Jaumann stress rate. The flow rule described above determines the direction of plastic straining and thus specifies the plastic Poisson ratio ν^p in a uniaxial compression test as a function of the yield surface ellipticity α, viz.

$$\nu^p = -\frac{\dot{\epsilon}^p_{11}}{\dot{\epsilon}^p_{33}} = \frac{\frac{1}{2} - \left(\frac{\alpha}{3}\right)^2}{1+\left(\frac{\alpha}{3}\right)^2}. \tag{4}$$

The dependence of ν^p upon α is shown graphically in Figure 5. Measured values of ν^p and deduced values of α from the measured ratio of the hydrostatic to the uniaxial strength are included in the figure, for the three foams. Good agreement between these experimental measurements and predictions is seen in support of the assumption of associated flow. It is tentatively suggested that measurement of ν^p in a uniaxial compression test is a quick and simple method for establishing the value of α and thereby the shape of the yield surface including the hydrostatic strength.

An equivalent strain rate $\dot{\hat{\epsilon}}$ which is the plastic work rate conjugate to $\hat{\sigma}$ is given by

$$\dot{\hat{\epsilon}}^2 = \left[1+\left(\frac{\alpha}{3}\right)^2\right]\left(\dot{\epsilon}_e^2 + \frac{1}{\alpha^2}\dot{\epsilon}_m^2\right). \tag{5}$$

It now remains to specify the hardening modulus $H(\hat{\epsilon}, \boldsymbol{\sigma})$. In general, H is homogeneous and of degree zero in stress state. Recall that for the case of uniaxial compression (or tension), the definitions of $\hat{\sigma}$ and $\dot{\hat{\epsilon}}$ have been normalised so that $\hat{\sigma}$ is the uniaxial stress and $\dot{\hat{\epsilon}}$ is the uniaxial plastic strain rate. We define $H \equiv \dot{\hat{\sigma}}/\dot{\hat{\epsilon}}$ to be the slope of the uniaxial Cauchy stress versus logarithmic plastic strain curve. This simplified self-similar model has been implemented by Chen [7] as a user-defined material constitutive law for the Finite Element code ABAQUS [8]. A more sophisticated hardening model where H is dependent on the stress path is given in Deshpande and Fleck [5].

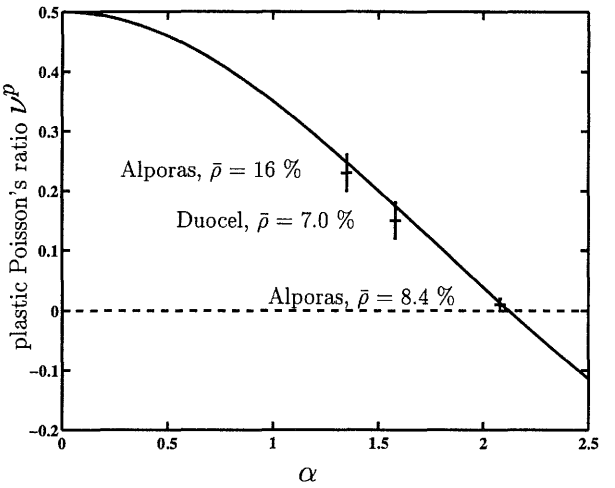

Figure 5: Comparison between measured Poisson's ratio value and that estimated assuming associated flow. The crosses denote the degree of uncertainty in experimental measurement.

5 Development of anisotropy

The isotropic model presented here is adequate for proportional stress paths. For non-proportional stress paths it may be necessary to consider anisotropic effects. An investigation into the development of anisotropy is discussed here. A sample of the high density Alporas was compressed uniaxially to a particular strain and the subsequent transverse strength, defined as the stress at 0.5 % offset strain was determined. The results are shown in Figure 5 where the ratio of the transverse strength σ_T to the current axial strength σ_A is plotted as a function of the nominal axial strain. Substantial anisotropy is seen to develop with the transverse strength nearly twice the current axial strength after the foam has been compressed uniaxially by 60 %.

Macroscopic straining occurs in the high density Alporas by the sequential collapse of spatially random bands. Figure 6 shows an initially uniform grid on a high density Alporas specimen after it has been deformed to an average 20 % compressive strain. The photograph clearly shows crush bands perpendicular to the direction of loading. These bands reinforce the foam in the transverse direction. A simple analysis to determine the transverse strength from the current axial strength follows.

Each crush band deforms to a strain ϵ_B before locking up. At lock-up a crush band has an isotropic strength σ_B and the undeformed part of the foam has an isotropic strength σ_A equal to the current axial strength of the foam. Since macroscopic straining occurs by the sequential collapse of crush bands, the macroscopic nominal strain ϵ is given by

$$\epsilon = \frac{n l_B \epsilon_B}{l_o}, \tag{6}$$

where n is the number of crush bands, l_B is the width of a crush band and l_o the specimen length. Assuming a plastic Poisson's ratio of zero, the volume fraction f of the crush bands

is

$$f = \frac{1-\epsilon_B}{\epsilon_B}\left(\frac{\epsilon}{1-\epsilon}\right). \tag{7}$$

By the rule of mixtures the transverse strength σ_T can be written as

$$\sigma_T = f\sigma_B + (1-f)\sigma_A. \tag{8}$$

Predictions of the transverse strength for the high density Alporas as a function of axial strain are shown by the solid line in Figure 5. ϵ_B is assumed to be the densification strain and taken as 0.8, and σ_B is the corresponding strength at densification equal to 13.5 MPa.

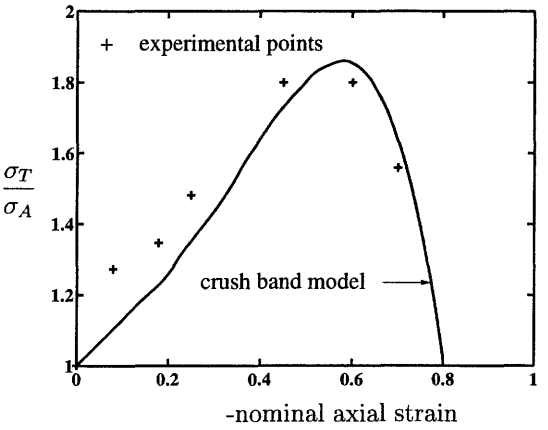

Figure 5: Ratio of the transverse to the axial strength as a function of compressive axial strain.

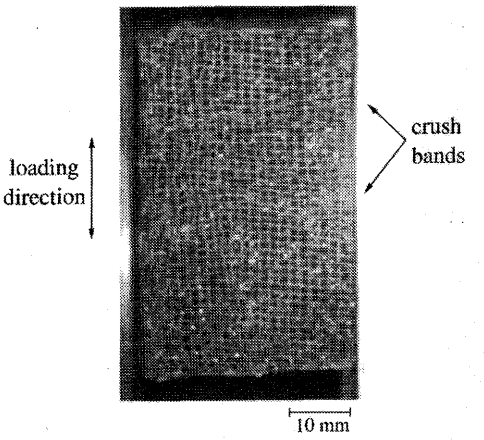

Figure 6: Deformed grid on an axially strained high density Alporas specimen.

6 Concluding remarks

A quadratic yield surface in mean stress-effective stress space is proposed for metallic foams in line with experimental observations. The hardening behaviour is calibrated against the uniaxial compressive response. However, experiments show that the hardening response is sensitive to the direction of the stress path and a more sophisticated hardening model has been developed [5]. Kinematic hardening models are required to account for the development of anisotropy, and are suggested as a topic for future study.

Acknowledgements

The authors are grateful to DARPA/ONR for their financial support through MURI grant number N00014-1-96-1028 on the Ultralight Metal Structures project at Harvard University.

References

[1] T C Triantafillou, J Zhang, T L Shercliff, L J Gibson, and M F Ashby. Failure surfaces for cellular materials under multiaxial loads- II: Comparison of models with experiment. *International Journal of Mechanical Sciences*, 31:665, 1989.

[2] G Gioux, T M McCormack, and L J Gibson. Failure of aluminium foams under multiaxial loads. Submitted to *International Journal of Mechanical Sciences*, 1998.

[3] R E Miller. A continuum plasticity model of the constitutive and indentation behaviour of foamed metals. Submitted to *International Journal of Mechanical Sciences*, 1998.

[4] M F Ashby, A G Evans, J W Hutchinson, and N A Fleck. Metal foams: A design guide. Technical Report CUED/C-MICROMECH/TR. 3, Cambridge University, Engineering Dept., 1998.

[5] V S Deshpande and N A Fleck. Isotropic constitutive models for metallic foams. Submitted to *Journal of Mechanics and Physics of Solids*, 1998.

[6] A-M Harte, N A Fleck, and M F Ashby. Fatigue failure of an open cell and a closed cell aluminium alloy foam. To appear in *Acta Metallurgica et Materialia*, 1999.

[7] C Chen. Manual for a UMAT user subroutine. Technical Report CUED/C-MICROMECH/TR.4, Dept. of Engineering, University of Cambridge, 1998.

[8] HKS. *ABAQUS/Standard users manual, Version 5.7.* Hibbit, Karlsson and Sorensen Inc., Providence, Rhode Island, 1997.